Studies in Surface Science and Catalysis 130
A. Corma, F.V. Melo, S.Mendioroz and J.L.G. Fierro (Editors)
© 2000 Elsevier Science B.V. All rights reserved.

Structure and Surface Properties of ZrO_2-Supported WO_3 Nanostructures

Chelsey D. Baertsch, Ryan D. Wilson, David G. Barton, Stuart L. Soled[a], and Enrique Iglesia

Department of Chemical Engineering, University of California at Berkeley, Berkeley, CA 94720; [a]Exxon Research and Engineering, Route 22 East, Annandale, NJ 08801

Isomerization reactions on ZrO_2-supported WO_x domains require catalyst pretreatment in air at high temperatures and the presence of H_2 during reaction. o-Xylene isomerization rates are proportional to H_2 pressure, suggesting a role of H_2 in reduction steps that form and maintain Bronsted acid sites. Consistent with this, O_2 reversibly inhibits isomerization reactions, apparently by titrating H atoms and re-oxidizing reduced W centers. NH_3 and pyridine adsorption showed that the Bronsted/Lewis acid site density ratio increases as WO_x surface density increases (3.6-17.7 W/nm^2). The total concentration of acid sites (per W-atom), however, decreases with increasing surface density as WO_x species become increasingly inaccessible with increasing cluster size. The effect of H_2 on the density and type of acid sites is much weaker than its effect on isomerization rates. Isomerization rates show a distinct maximum near monolayer WO_x coverages on ZrO_2 (10 W/nm^2) whether the rates are normalized by W-atoms, BET surface area, or acid site density. The Bronsted acid sites responsible for o-xylene isomerization (in H_2) appear to be present as a small fraction of those titrated by NH_3 or pyridine. Such sites are unusual in that they are rendered inactive by small amounts of oxygen and show higher turnover rates than Bronsted acids on H-ZSM5.

1. INTRODUCTION

Zirconia-supported WO_3 (WO_x-ZrO_2) catalyzes n-butane and n-pentane isomerization at ~300 K after treatment in air at 1073 K [1]. These materials also catalyze n-heptane conversion to isoheptanes with high selectivity with H_2 in the reactant stream and Pt clusters on the catalyst surface [2]. Several studies have reported a marked effect of treatment temperature on the structure and catalytic properties of WO_x-ZrO_2, and the presence of two-dimensional polytungstates appears to be required for efficient acid catalysis. Maximum isomerization rates at intermediate treatment temperatures or W concentrations have been reported for the isomerization of n-pentane [1, 3, 4] and o-xylene [5, 6]. The treatment temperature required for maximum rates increases with decreasing W concentration, and o-xylene isomerization rates (per W-atom) depend only on the WO_x surface density, reaching a maximum at ~10 W/nm^2, irrespective of the W concentration or treatment temperature [5, 6].

Characterization of WO_x-ZrO_2 with Raman, UV-visible, and X-ray absorption [5, 6, 7] showed that the structure and domain size of WO_x-ZrO_2 nanostructures also depend only on WO_x surface density, irrespective of whether it is achieved by changing the W concentration or the treatment temperature (surface area). Inactive monotungstate species exist at low WO_x surface densities (<4 W/nm^2). As the surface density increases (to ~10 W/nm^2), monotungstate species condense into two-dimensional polytungstate domains, which catalyze o-xylene isomerization at 523 K. At higher surface densities, excess WO_x forms WO_3 clusters

with lower surface area and lower catalytic activity. X-ray absorption near-edge spectra showed that WO_x structures retain the distorted octahedral structure characteristic of bulk WO_3 at all surface densities [5, 6, 7]. UV-visible spectroscopy showed that reduced (color) centers form in the presence of H_2 at 523 K only on WO_x-ZrO_2 catalysts with surface densities above 4 W/nm^2 [7]. The rate of formation of reduced centers increased with increasing WO_x surface density. Large WO_3 crystallites are poorly dispersed and reduce with the removal of oxygen as H_2O, resulting in inactive WO_{3-x} species. This study investigates the role of H_2 on the formation of acid sites and the effect of WO_x surface density on the density and nature of these acid sites.

2. EXPERIMENTAL METHODS

WO_x-ZrO_2 was prepared by methods previously reported [1, 2]. High surface area zirconia oxyhydroxide ($ZrO_x(OH)_{4-2x}$) was prepared by precipitation of 0.5 M zirconyl chloride solutions ($ZrOCl_2{\cdot}8H_2O$, Aldrich, >98 wt.%) with NH_4OH at a constant pH of 10. Precipitates were filtered and washed in order to remove Cl^-, and then dried at 383 K. $ZrO_x(OH)_{4-2x}$ was impregnated with $(NH_4)_6H_2W_{12}O_{40}$ solutions to incipient wetness, and then treated in dry air at 773-1273 K. Pt/WO_x-ZrO_2 (0.3 wt. % Pt) was prepared by impregnation of WO_x-ZrO_2 with a solution of tetraamine platinum hydroxide, dried at 383 K, and then treated in air at 723 K. Pure ZrO_2 samples were treated in dry air at 773 K to preserve the tetragonal phase that is present in WO_x-ZrO_2 samples even at higher treatment temperatures.

Chemisorption uptakes were measured using a Quantachrome 1C Autosorb apparatus. Samples were dehydrated in He at 673 K for 4 h and evacuated at 313 K before CO_2 isotherms (2.7-53 kPa). CO_2 uptakes were calculated by extrapolating to zero pressure to subtract weakly adsorbed CO_2. H_2 uptakes were measured at 523 K and 80 kPa after in-situ air calcination. Multipoint BET isotherms were obtained by N_2 physisorption at 77 K using a Quantasorb surface area analyzer after evacuation at 473 K for 2 h. Measured BET surface areas correlated with crystallite sizes calculated from XRD results [6, 7].

A Harrick Scientific diffuse reflectance attachment (DRP-XXX) and in-situ cell (HVC-DR2) were used to obtain diffuse reflectance infrared spectra (Mattson RS-10000 FTIR). Powders were placed on a porous quartz frit and gases flowed through the powders. WO_x-ZrO_2 samples were dehydrated in dry air (Matheson, Zero) at 773 K for 1 h, then treated in He or H_2 (Matheson, UHP) at 523 K for 1 h. The pretreatment in H_2 at 523 K, used throughout this study, is intended to replicate the conditions used in catalytic studies. NH_3 was chemisorbed at 298 K using 0.93% NH_3 in He (Altair, certified standard) diluted with equal parts of Ar or H_2. Pyridine (Aldrich, 99.8%) was adsorbed at 298 K by injection into a H_2 or He carrier stream. Spectra of adsorbed NH_3 and pyridine were acquired at 298-773 K after purging the cell with pure H_2 or Ar. Intensities are reported in apparent absorbance units [8], using the dehydrated sample before chemisorption of titrants as the reference.

Temperature-programmed NH_3 desorption was carried out after treating WO_x-ZrO_2 (~1 g) at 773 K in dry air for 1 h and then in Ar or H_2 at 523 K for 1 h. NH_3 was adsorbed (1 h, 298 K) using 0. 93% NH_3 in He (0.833 cm^3 s^{-1}) mixed with Ar or H_2 (0.833 cm^3 s^{-1}). NH_3 was desorbed in 0.833 cm^3 s^{-1} Ar by increasing the temperature at 0.17 K/s to 973 K and measuring the intensity at 16 amu with a Leybold-Inficon mass spectrometer.

o-Xylene isomerization was carried out in a single pass flow reactor and a recirculating batch reactor at 523 K [5, 9]. Reactants and products were analyzed by gas chromatography (Hewlett-Packard 5890 GC, DB-WAX capillary column, flame ionization

detector). Catalysts were treated in flowing air at 773 K for 1 h and reduced in flowing H_2 at 523 K with the H_2 pressure used during reaction in order to avoid initial transients caused by gas-surface re-equilibration during catalysis. Batch reactor studies were conducted at 0.67 kPa o-xylene (NBS, >99.995%) and 106 kPa H_2, and operated at <2% conversion per pass. In the flow reactor, o-xylene (Reidel De Haen, > 99%) was introduced through an atmospheric thermostated saturator. Initial reaction rates were determined by linear extrapolation of semi-logarithmic plots of reaction rates vs. time. Catalytic oxygen titrations were carried out by syringe injection of air (~0.1 cm^3) into the reactant stream.

3. RESULTS AND DISCUSSION

3.1 o-Xylene Isomerization Studies

The effect of H_2 on initial isomerization rates was measured by varying the H_2 pressure between 0 and 128 kPa at 0.67 kPa o-xylene and 523 K (Table 1). Initial isomerization rates increased linearly with H_2 pressure, but para/meta isomer ratios were not affected by H_2. This suggests that H_2 affects only the density of the acid sites and not their strength, because an increase in acid strength would lead to longer surface residence times of adsorbed xylenes and to higher para/meta isomer ratios. A detailed analysis of o-xylene isomerization kinetics [9] showed that H_2 effects reflect the formation of Bronsted acid sites via H_2 dissociation and migration to WO_3 domains, which draw electron density away from H-atoms to form $H^{\delta+}$ sites. A pulse of O_2 (0.147 O-atoms/W-atom) added to the reactant stream led to the immediate, but temporary, elimination of catalytic activity (Figure 1). o-Xylene isomerization rates recover within the same characteristic time observed when WO_x- ZrO_2 catalysts were exposed to H_2/xylene reactants without pre-reduction at 523 K [9]. The reversible titration of Bronsted acid sites by O_2 appears to involve the reaction of oxygen with H-atoms (forming H_2O) on WO_x domains. Clearly, active sites on WO_x-ZrO_2 possess unique redox properties, unexpected for conventional acidic oxides, and the density of such acid sites is low (<0.295 $H^{\delta+}$ sites/W-atom). Using the catalytic titration of n-pentane isomerization with 2,6-dimethylpyridine, a sterically hindered probe that titrates only Bronsted acid sites, Santiesteban *et al.* showed that the density of Bronsted acid sites on WO_x-ZrO_2 is very low (0.0024 strong H^+ sites/W-atom, 0.0115 total H^+ sites/W-atom) [4].

Table 1 : Effect of H_2 Pressure on Initial o-Xylene Rates (15% WO_3-ZrO_2, 46 m^2/g, 8.4 W/nm^2)

H_2 Pressure (kPa)	Initial Isomerization Rate (10^{-3} s^{-1} per W-atom)
0.00	0.33
9.82	0.42
25.90	0.55
52.90	1.02
92.70	1.69
127.40	2.25

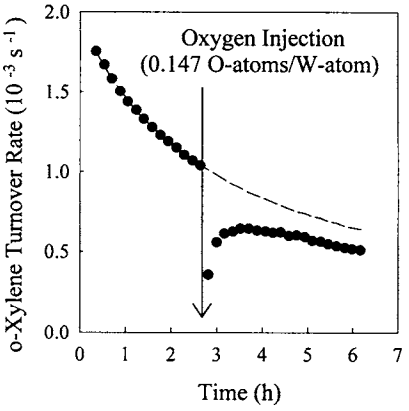

Figure 1: Catalytic O_2 Titration of o-Xylene Isomerization (15% WO_3-ZrO_2, 46 m^2/g, 8.4 W/nm^2)

3.2 Diffuse Reflectance Infrared Spectroscopy (DRIFTS) of Adsorbed Titrants

DRIFTS of chemisorbed NH_3 and pyridine was used to distinguish Bronsted and Lewis acid sites on WO_x-ZrO_2 and to explore the effects of H_2 and WO_x surface density on the density of such acid sites. Only the results of NH_3 adsorption studies are presented here; similar conclusions were reached using pyridine as the titrant. Figure 2 shows spectra of NH_3 adsorbed on WO_x-ZrO_2 (9.6 W/nm^2) at 298-623 K using Ar as the carrier. The bands at 1222 cm^{-1} (δ_s) and 1598 cm^{-1} (δ_{as}) at 298 K correspond to NH_3 coordinated to Lewis (L) acid sites, and the bands at 1439 cm^{-1} (δ_a) and 1661 cm^{-1} (δ_s) to NH_4^+ on Bronsted (B) acid sites [10-12]. The weak shoulder at ~1120 cm^{-1} (δ_s) reflects traces of hydrogen-bonded NH_3, which desorbs readily at ~373 K. As temperature increases, the band at 1439 cm^{-1} (B) shifts to lower frequency, the band at 1222 cm^{-1} (L) shifts to higher frequency, and the band at 1661 cm^{-1} (B) disappears at ~523 K. These changes indicate that the NH_3 binding energy on Bronsted sites is lower than on Lewis sites. Pure ZrO_2 shows only N-H deformation bands at 1164 cm^{-1} (δ_s) and 1598 cm^{-1} (δ_{as}) at 298 K (not shown), corresponding to Lewis acid sites. A previous infrared study also detected Lewis acid sites on ZrO_2 [13]. The 1164 cm^{-1} band (L) on ZrO_2 shifts to higher frequency when WO_x is present, suggesting an increase in Lewis acid strength, which may be caused by the lower electron density of W^{6+} compared to Zr^{4+}. Also, the WO_x surface density (domain size) did not influence the frequency of any bands, suggesting that the acid strength and the W oxidation state do not change with WO_x surface density, a conclusion consistent with previous studies [5, 6, 7, 9]. Bronsted and Lewis acid sites have been reported on a series of WO_x-ZrO_2 catalysts using pyridine and low temperature CO adsorption [14-16], but the effects of H_2 and WO_x surface density were not examined.

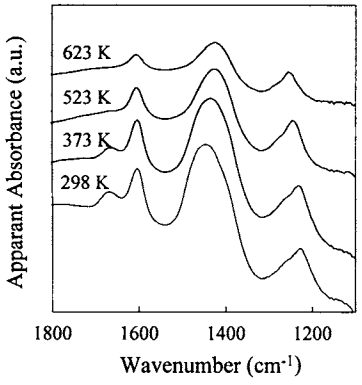

Figure 2: Infrared Spectra of NH_3 Adsorption on WO_x-ZrO_2 (30% WO_3, 81 m^2/g, 9.6 W/nm^2)

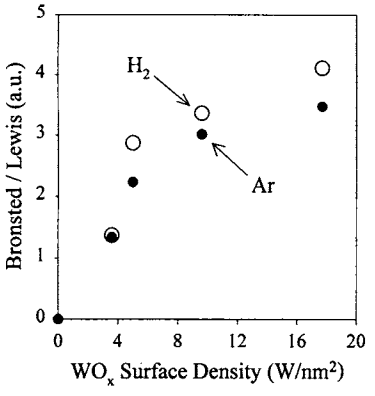

Figure 3: Bronsted/Lewis Acid Site Density Ratio at 523 K after Ar and H_2 Pretreatments

Figure 3 shows the relative ratio of Bronsted/Lewis acid site densities at 523 K in both Ar and H_2 for WO_x-ZrO_2 (0, 3.9, 9.6, and 17.7 W/nm^2) and for Pt/WO_x-ZrO_2 (5.0 W/nm^2) calculated from the areas under the 1420 cm^{-1} (B) and the 1241 cm^{-1} (L) bands. Bronsted/Lewis acid site ratios increased with increasing WO_x surface density up to the theoretical polytungstate monolayer value (~8 W/nm^2), and then began to level off as WO_x surface density increased further. The infrared cross section of NH_3 adsorbed on B and L sites would be required to quantify the ratio shown in Figure 3 and to distinguish an increase in the number of B sites from a decrease in the number of L sites as the cause of changes in their ratio. Nonetheless, it appears that WO_x clusters possess the Bronsted acidity, possibly as tungsten bronze (H_xWO_3) or as hydroxyls on monotunsgtate and polytungstate Zr-O-W linkages. The presence of H_2

(50.7 kPa) during NH_3 adsorption at 523 K and infrared measurements (101.3 kPa) lead to larger Bronsted/Lewis acid site ratios (Figure 3), except for samples with less than 4 W/nm^2, which also showed no reduction in H_2 at 523 K by UV-visible spectroscopy [7]. The effects of H_2, however, are weak and possibly within the accuracy and reproducibility of the measurements. In any case, the effects of H_2 on the surface acid properties are, if present at all, much weaker than the observed effects of H_2 on o-xylene isomerization rates. Also, the presence of Pt does not enhance the Bronsted/Lewis acid site ratio, an effect that was reported on Pt/SO_x-ZrO_2 and attributed to the conversion of Lewis sites into Bronsted sites by H_2 [17]. Thus, if H_2 indeed converts Lewis acid sites into Bronsted acid sites on WO_x-ZrO_2, the density of these Bronsted acid sites is much smaller than the total acid site density detected by adsorbed NH_3.

3.3 Temperature Programmed Desorption of Ammonia (NH_3 TPD)

The combined density of Bronsted and Lewis acid sites on WO_x-ZrO_2 was determined from the amount of adsorbed NH_3 that desorbed during heating from 298 K. WO_x-ZrO_2 (0-12.1 W/nm^2) was studied after pretreatment and NH_3 adsorption in either Ar or H_2. WO_x-ZrO_2 samples, which showed Bronsted and Lewis acid sites, and pure ZrO_2, which showed only Lewis acid sites, gave similar desorption profiles, with a peak at about 423 K, and at least two broader peaks between 500 and 800 K. Chemisorption of CO_2, which binds to the basic sites of ZrO_2 but not to WO_x domains [18], was used to determine the ZrO_2 surface area that remains exposed in WO_x-ZrO_2 [7]. These data were then used to correct NH_3 uptakes for adsorption on ZrO_2 acid sites. The corrected NH_3 uptakes are shown in Figures 4a and 4b after either H_2 or Ar pretreatments. NH_3 uptakes per surface area (Figure 4a) increased with increasing WO_x surface density until the monotungstate saturation coverage was reached (~4 W/nm^2), indicating a stepwise deposition of well dispersed monotungstate WO_x species. At higher surface densities, the areal densities of acid sites reached constant values. The acid site density per W-atom (Figure 4b) decreased monotonically with increasing surface density as WO_x species become increasingly inaccessible to NH_3 due to the growth of WO_3 domains. H_2 does not influence the measured acid site densities, but the conversion of Lewis into Bronsted acid sites by H_2 would not change the total number of acid sites detected by adsorbed NH_3.

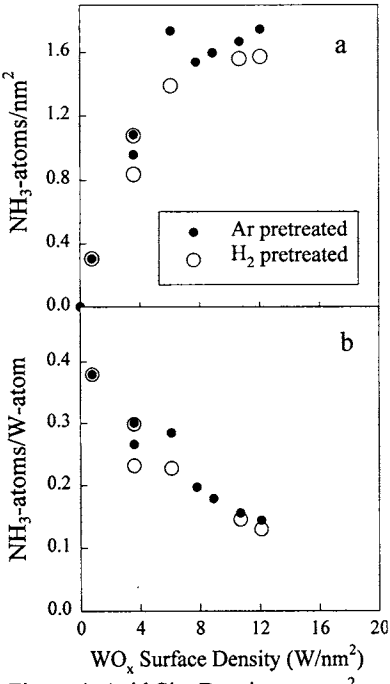

Figure 4: Acid Site Density per nm^2 (a) and per W-atom (b) as a Function of WO_x Surface Density

o-Xylene isomerization rates, normalized by the number of W-atoms [5] or by the BET surface area, show a sharp maximum at intermediate WO_x surface densities. Figure 5 shows initial o-xylene isomerization rates (in H_2, 106 kPa) normalized by the number of acid sites obtained from corrected NH_3 uptakes. Clearly, changes in the total acid site density do not account for the effects of WO_x surface density on isomerization rates. H_2 uptakes on WO_x-ZrO_2 (0-17 W/nm^2) at 523 K, however, seem to correlate with o-xylene isomerization rates, with a maximum uptake of ~0.06 H-atoms/W-

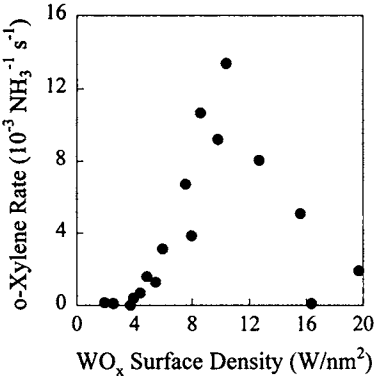

Figure 5: o-Xylene Isomerization Rates per Acid Site

Table 2: o-Xylene Rates for WO_x-ZrO_2 and H-ZSM5

	Initial Isomerization Turnover Rate (10^{-3} s^{-1})	
	per W or Al-atom	per Bronsted acid site*
WO_x-ZrO_2 (8.4 W/nm^2)	1.7	26
H-ZSM5 (14.5 Si/Al)	1.8	1.8

[124 kPa H_2, 523 K]
* per chemisorbed H-atom on WO_x-ZrO_2

atom on monolayer WO_x-ZrO_2. H_2 uptakes also confirm the low density of acid sites responsible for the very high o-xylene isomerization turnover rates. The unique Bronsted acid sites formed from H_2 on WO_x-ZrO_2 are much more active than zeolitic Bronsted acid sites (Table 2) [4], and differ significantly in their nature in that they require H_2 in a reversible fashion, apparently for the generation of colored centers normally associated with H_xWO_3. Kinetic studies of o-xylene isomerization on WO_x-ZrO_2 are consistent with a Bronsted acid catalyzed mechanism in which intramolecular 1,2 methyl shifts occur after protonation, and Lewis acid sites can only act as stoichiometric deactivation sites [9].

REFERENCES

1. Hino, M. and Arata, K., J. Chem. Soc. Chem. Commun., 1259 (1987).
2. Iglesia, E., Barton, D., Soled, S., Miseo, S., Baumgartner, J., Gates, W., Fuentes, G., and Meitzner, G., Stud. Surf. Sci. Catal. 101, 533 (1996).
3. Larsen, G. and Petkovic, L., Appl. Catal. A 148, 155 (1996).
4. Santiesteban, J.G., Vartuli, J.C., Han, S., Bastian, R.D., and Chang, C.D., J. Catal. 168, 431 (1997).
5. Barton, D.G., Soled, S.L., and Iglesia, E., Topics in Catal. 6, 87 (1998).
6. Barton, D.G., Soled, S.L., Meitzner, G.D., Fuentez, G.A., and Iglesia, E., J. Catal. 181, 52 (1999).
7. Barton, D.G., Shtein, M., Wilson, R.D., Soled, S.L., and Iglesia, E., J. Phys. Chem. B 103, 630 (1999).
8. Rajagopal, S., Marzari, J.A., and Miranda, R., J. Catal. 151, 192 (1995).
9. Wilson, R.D., Barton, D.G., and Iglesia, E., Submitted to J. Catal. (1999).
10. Mapes, J.E. and Eischens, R.P., J. Phys. Chem. 58, 1059 (1954).
11. Echterhoff, R. and Knozinger, E., Surf. Sci. 230, 237 (1990).
12. Ramis, G., Cristiani, C., Elmi, A., and Pierluigi, V., J. Mol. Catal. 61, 319 (1990).
13. Yamaguchi, T., Nakano, Y., and Tanabe, K., Bulletin of the Chemical Society of Japan 51 (9), 2482 (1978).
14. Larsen, G., Raghavan, S., Marquez, M., and Lotero, E., Catal. Lett. 37, 57 (1996).
15. Boyse, R.A. and Ko, E.I., J. Catal. 171, 191 (1997).
16. Scheithauer, M., Cheung, T.-K., Jentoft, R.E., Grasseli, R.K., Gates, B.C., and Knozinger, H., J. Catal. 180, 1 (1998).
17. Ebitani, K., Konishi, J., and Hattori, H., J. Catal. 130, 257 (1991).
18. Vaidyanathan, N., Houalla, M., and Hercules, D.M., Catal. Lett. 43, 209 (1997).